INTL JOURNAL OF ELECTRONICS AND TELECOMMUNICATIONS, 2020, VOL. 66, NO. 4, PP. 745–752
Manuscript received January 17, 2020; revised October, 2020. DOI: 10.24425/ijet.2020.134036

Start Acceleration of the Space GPS Receiver

Pavel Kovář

***Abstract*—The cold start of the space GPS receiver, i.e. the start without any information about the receiver position, satellite constellation, and time, is complicated by a large Doppler shift of a navigation signal caused by the satellite movement on the Earth orbit. That increases about five times the search space of the navigation signals compared to the standard GPS receiver. The paper investigates a method of the acceleration of the GPS receiver cold start time designed for the pico- and femto-satellites. The proposed method is based on a combination of the parallel search in Doppler frequency and PRN codes and the serial search in code phase delay. It can shorten the cold start time of the GPS receiver operating on LEO orbit from about 300 to 60 seconds while keeping the simplicity of FPGA signal processor and low power consumption. The developed algorithm was successfully implemented and tested in the piNAV GPS receiver. The energy required for the obtaining of the position fix was reduced five times from 36 on to 7.7 Joules. This improvement enables applications of such receiver for the position determination in smaller satellites like Pocket Cube or femto-satellites with a lower energy budget than the Cube Satellite.**

***Keywords*—FPGA, navigation, low earth orbit, acquisition accelerator**

I. Introduction

PICO- and femto-satellites are cost-effective satellites for space research, remote sensing, and technology testing on the Earth orbit. Most physical measurements in the space environment and the Earth remote sensing require precise knowledge of the satellite position and time. The precision position information of the satellite is essential for energy savings. The GPS receiver is commonly seen as a suitable sensor for satellite position determination achieving several meters precision [1], [2]. The paper deals with the operation of the GPS receiver usable for Low Earth Orbit (LEO) small or pico- and femto-satellites from the cold start point of view, which means the beginning of the receiver operation without prior knowledge about the position, time, visible satellites, and navigation satellites data.

The miniaturized satellites have to deal with a tight energy budget because of a small area of solar panels. For instance, the average power budget of simple 1U Cube satellite (size 100x100x100 mm and weight approximately 1 Kg) is approx. 1 Watt [3]. Moreover, most of these satellites are unstabilized or use a very primitive stabilization system, which means that these satellites can even slowly rotate during its operation.

The preparation of this document was supported from the European Regional Development Fund-Project CRREAT No. CZ.02.1.01/0.0/0.0/15 003/0000481.

P. Kovář is with Faculty of Electrical Engineering, The Czech Technical University in Prague, Prague, The Czech Republic (e-mail: kovar@fel.cvut.cz).

The conditions for the GPS receiver operation on the LEO orbit are rather different in comparison with the operating conditions of a standard GPS receiver on the ground [1], [2]. The signal propagation is much simpler. There are no obstacles and objects that block, attenuate, and reflect navigation signals. On the other hand, the speed of movement of the LEO satellite is about 8 km/s, so the Doppler shift of the navigation signals is much larger than on the ground [4]. The LEO satellite GPS receiver is also exposed to radiation [5].

GPS system is based on a ranging method [6], [7] where the user position is calculated from measured propagation delays of the navigation signals between the navigation satellites and user receiver. The position velocity and time (PVT) determination algorithm also needs navigation satellite positions. The navigation signal is specially designed for high precision measurement of the time of arrival. The carrier frequency is modulated by so-called ranging code that is featured with a narrow peak of an auto-correlation function. This modulation method is called direct sequence spread spectrum (DSSS).

The signal processing method of the GPS signals in the receiver is based on a correlation reception method. The receiver calculates cross-correlation function between a received signal and a replica signal generated in the receiver and tries to synchronize the replica signal to the received signal ranging code delay and Doppler frequency. The signal processing is divided into two problems: initial synchronization (called signal acquisition) and signal tracking.

The cold start of the navigation receiver consists of

1) Acquisition of the signal of at least four satellites
2) Reception of the ephemeris of the tracked satellites
3) Computation of the user position

The signal acquisition was identified as a most critical GPS operation on the Earth orbit, therefore the paper focuses on the analyses and solution of this problem because the duration of the ephemeris reception cannot be shorted by the user receiver.

From the mathematical point of view, the signal acquisition is a determination of the maximum of two-dimensional (ranging code delay and Doppler frequency shift) cross-correlation function (Fig. 1). The dimension of the search space in which the maximum can be located is analyzed in section II. The analysis of the acquisition sensitivity then follows. The rest of the paper deals with the implementation issues and tests of the selected algorithm in the designed piNAV GPS receiver.

II. Study of the Doppler Shift of the Navigation Signal on LEO Orbit

The acquisition complexity depends on the dimension of the search space and sensitivity, i.e. minimal detectable signal level [7].

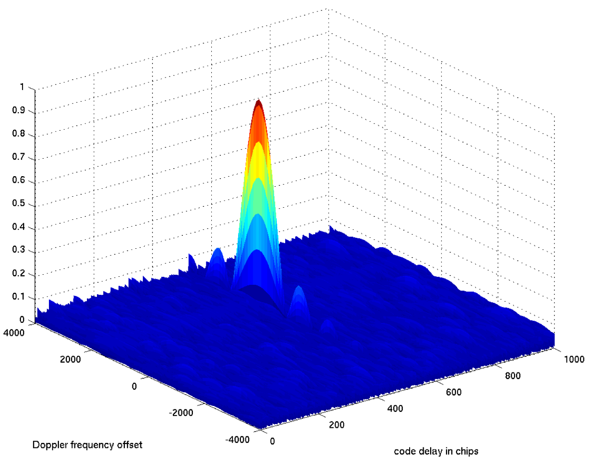

Fig. 1. Two-dimensional correlation function of GPS L1 signal.

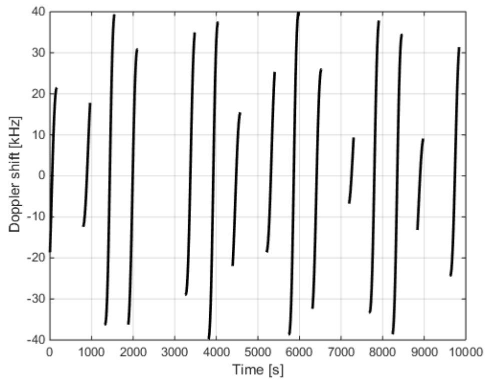

Fig. 2. Doppler shift of GPS L1 signal measured on LEO orbit.

The dimension of the search space in the delay is defined by the period of the PRN code that is one millisecond for GPS L1 signal. The dimension in frequency depends on the Doppler frequency caused by the user movement and maximal error of the navigation receiver frequency standard. A typical value of the search space in frequency is +/-8 kHz for a ground use of a standard GPS receiver in which the main contribution is the navigation satellite movement [7], [8].

The Doppler frequency shift of the signal measured in the LEO satellite is dramatically larger due to the orbital speed of the LEO satellite that is approximately 8 km/s [4]. The typical progress of the Doppler frequency of GPS L1 navigation signals measured on LEO orbit is on Fig. 2. The gaps in Doppler shift curves represent cases when the navigation satellite is below the horizon and its navigation signal is not available.

The maximal search space in frequency is approximate +/- 50 kHz. Fig. 3 shows that within such interval, we can use most of the visible satellites and a sufficient number of the satellites can be visible with substantially lower Doppler shift. Therefore, the LEO satellite navigation receiver can investigate narrower search space in frequency than the maximal space for a reliable cold start. The search space in frequency should be set to the value that guarantees the reliable acquisition of at least four satellites. This step dramatically saves computation complexity of the cold start which leads to the shorter cold start time.

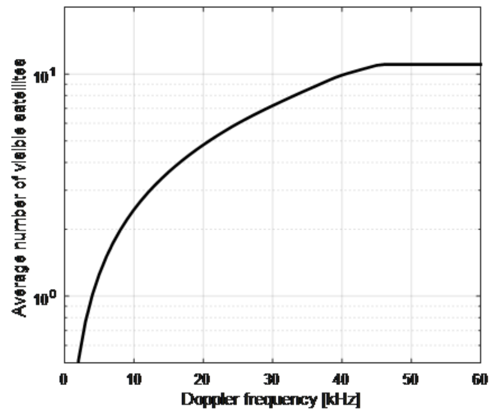

Fig. 3. Average number of visible satellites that have Doppler frequency shift not exceeding given value.

The optimization of the search space in frequency for LEO satellite receiver with implemented serial search algorithm is in [8]. The optimum value is +/- 35 kHz. The optimization criterion was cold start time. The optimal search space of the LEO satellite GPS receiver is approximately 4 times wider than the search space used in standard GPS receiver.

On the other hand, the space GPS receiver processes uninterrupted navigation signals, while navigation signals on the ground could be attenuated or blocked by various obstacles. Therefore, the processing gain of the ground receiver should be higher than the processing gain of the space receiver to be able to compensate signal blockage.

III. Signal Acquisition Method

The signal acquisition is finding the maximum of the likelihood function $L(\tau_i, \omega_d)$ in code delay τ_i and Doppler frequency shift ω_d [7].

$$(\hat{\tau}_i, \hat{\omega}_i) = \arg\max_{\tau_i, \omega_d} L(\tau_i, \omega_d) \tag{1}$$

The likelihood function is in our case equal to the modulus $|\mathrm{R}_{s,r}(\tau_i, \omega_d)|$ or modulus power $|\mathrm{R}_{s,r}(\tau_i, \omega_d)|^2$ of cross-correlation function between received signal and replica signal. The dimension of the search space in Doppler frequency was discussed above. The dimension in code delay is one period of PRN code. The acquisition algorithm samples the correlation function in code delay τ_i and Doppler frequency shift ω_d. The element of the search space is called a search cell.

The acquisition algorithms are classified as:

- Serial search algorithms that investigates search space cell by cell, so the receiver computes cross-correlation function for one search cell consecutively.

- Parallel search algorithms that are capable of calculating cross-correlation function for a larger number of search cells in one step.

The performance of the signal acquisition algorithm is measured by the signal detection probability P_d. It is the probability that the value of cross-correlation function in the cell with correlation maximum is higher than the values of the cross-correlation function for the rest cells of the search space.

The problem will be solved for additive white Gauss noise (AWGN) channel because this channel model is typical for space radio links. The probability density function of the correlation envelope in a cell with correlation maximum has the Rayleigh-Rice distribution

$$p_s\left(x\right)=\begin{cases}\frac{x}{\sigma_n^2}e^{-\frac{x^2+A^2}{2\sigma_n^2}}I_0\left(\frac{xA}{\sigma_n^2}\right) & x\geq 0\\ 0 & \text{outside}\end{cases} \tag{2}$$

where A is an amplitude of the usual signal on the correlator output, σ_n is a standard deviation of the noise and I_0 is modified Bessel function of the first kind.

The probability density function of the cross-correlation envelope in the cell outside the correlation maximum has the Rayleigh distribution

$$p_n\left(x\right)=\begin{cases}\frac{x}{\sigma_n^2}e^{-\frac{x^2}{2\sigma_n^2}} & x\geq 0\\ 0 & \text{outside}\end{cases} \tag{3}$$

The probability of detection (finding proper correlation maximum) in search space of dimension N_c cells is given

$$P_{d\,N_c}\left(A,\sigma_n,N_c\right)=\int_0^\infty p_s\left(x\right)\left(\int_0^x p_n\left(z\right)dz\right)^{N_c-1}dx=$$
$$=\int_0^\infty\frac{x}{\sigma_n^2}e^{-\frac{X^2+A^2}{2\sigma_2^n}}I_0\left(\frac{xA}{\sigma_n^2}\right)\left(1-e^{-\frac{x^2}{2\sigma_n^2}}\right)^{N_c-1}dx \tag{4}$$

The amplitude A of the signal can be expressed with the help of commonly used carrier to noise ratio

$$A=\sigma_n\sqrt{2\cdot 10^{\frac{\frac{C}{N_0}-10\log T_I}{10}}} \tag{5}$$

T_I is a coherent integration time and $\frac{C}{N_0}$ is a carrier to spectral noise density.

The sensitivity of signal detection depends on T_I. Unfortunately, there are physical and technical limits for its prolongation. One of the limit factors is not considering of the navigation message. The most common setup is $T_I=1$ milliseconds, which is the period of ranging code. The problem of this setup is relatively poor sensitivity, i.e. that high probability of signal detection is achieved for high $\frac{C}{N_0}$.

One of the methods to improve signal detection sensitivity is to use a non-coherent summing or averaging of the modulus or power of the cross-correlation function. The likelihood function can be expressed in this case

$$L_N\left(\tau_i,\omega_d\right)=\sum_{i=1}^{N}\left|R_{s,r}\left(\tau_i,\omega_d\right)\right| \tag{6}$$

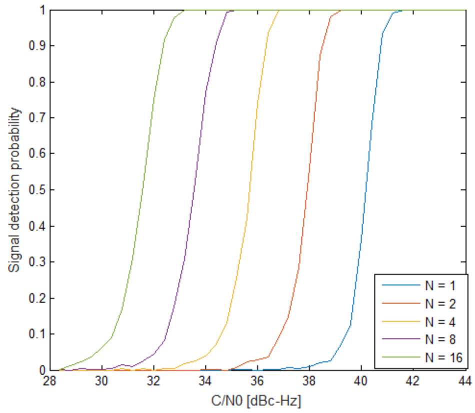

Fig. 4. Probability of detection for GPS L1 signal, T_I=1 ms, N_c=128000 cells.

The derivation of the signal detection probability for non-coherent summing of the cross-correlation function is rather complicated. However, for a large number of summing N, the central limit theorem can be applied. The probability density function $L_N(\tau_i,\omega_d)$ converges to the probability density function of the normal distribution. The detection probability under this assumption is

$$P_{dNN_c}\left(A,\sigma_n,N,N_c\right)=\int_{-\infty}^{\infty}\frac{1}{\sigma_{N_S}\sqrt{2\pi}}e^{-\frac{x-}{2\sigma^2_{N_S}}}$$
$$\left(\int_{-\infty}^{x}\frac{1}{\sigma_{N_n}\sqrt{2\pi}}e^{-\frac{\left(z-\mu^2_{N_n}\right)^2}{2\sigma^2_{N_n}}}dz\right)^{N_c-1}dx \tag{7}$$

Where $\mu_{Nn}=N\sigma_n\sqrt{\frac{\pi}{2}}$ and $\sigma^2_{Nn}=N\sigma_n^2\frac{4-\pi}{2}$ are average value and variance of $L_N\left(\tau_i,\omega_d\right)$ in a non-maximum cell, and $\mu_{Ns}=N\sigma_n\sqrt{\frac{\pi}{2}}L_{\frac{1}{2}}\left(\frac{A^2}{2\sigma_n^2}\right)$ and $\sigma^2_{Nn}=N\left(2\sigma_n^2+A^2-\frac{\pi\sigma_n^2}{2}L^2_{\frac{1}{2}}\left(\frac{-A}{2\sigma_n^2}\right)\right)$ are average value and variance of $L_N\left(\tau_i,\omega_d\right)$ in a maximum cell. $L_n\left(x\right)$ is Laguerre polynomial.

The analytical evaluation of the (7) is rather complicated, therefore the numerical results were obtained by computer simulation (Fig. 4). The used dimension of the search space covers whole code delays (2000) and 64 frequencies that correspond to the frequency search range +/- 32 kHz.

It is clear from Fig. 4. that non-coherent summation improves acquisition sensitivity, i.e. that the required probability of signal detection is reached for a lower signal to noise ratio.

The real performance of the acquisition unit is several dB worse due to the various implementation losses, for example, loss of the signal to noise ratio caused by the quantization of the signal in receiver or loss caused by the sampling of the cross-correlation function outside the maximum.

The analysis was done under assumption that the receiver processes the signal in a given cell for the fixed predefined time, for example, it calculates cross-correlation function on time intervals one millisecond and creates non-coherent sums for eight consecutive time intervals, so the receiver processes eight milliseconds of the signal for each cell. The search rate is then defined by the ratio of the number of cells that are investigated in parallel N_P and processing time

$$v_s = \frac{N_p}{T_I N} \tag{8}$$

A. Serial search method

The serial search method investigates the search space consecutively cell by cell therefore, the fixed processing time is not necessary. The significant improvement can be reached by the usage of the variable processing time of the search cell [7], [8]. The decision process can have more stages. In the first stage, we can process the signal within one millisecond interval and then decide whether the further investigation of particular search cell will be rejected due to the low value of the correlation envelope or whether it will continue in the next stage of the decision process for a longer time.

The first stage probability of detection is equal to a probability that the correlation envelope in the cell with correlation maximum exceeds threshold V_t and can be expressed as

$$P_{dt} = \int_{V_t}^{\infty} p_s(x)\, dx \tag{9}$$

Probability of the false alarm, i.e. the probability that signal in the cell outside the correlation maximum exceeds threshold V_t is

$$P_{fat} = \int_{V_t}^{\infty} p_n(x)\, dx \tag{10}$$

The threshold V_t is set to the value so that the probability of the signal detection will be high (close to 1). If the integration time T_I is not sufficient, the probability of false alarm is high, so the receiver detects the signal in the incorrect cell, which is unwanted. Fortunately, the receiver can use a confirmation algorithm for compensation of this problem.

There are two well-known confirmation algorithms, M of N and Tong algorithms. If the signal in the cell is detected, the M of N algorithm remains in the cell for N periods of T_I and detects, how many times the threshold V_t is exceeded. If the threshold is exceeded at least M times, the signal is detected, otherwise the receiver continues in the investigation of the next cell.

The overall probability of signal detection by implementing M of N algorithm is

$$P_{dNM} = P_{dt} \sum_{n=M}^{N} \binom{N}{n} P_{dt}^{n} \left(1 - P_{dt}\right)^{N-n} \tag{11}$$

The overall probability of thr false alarm is

$$P_{faNM} = P_{fat} \sum_{n=M}^{N} \binom{N}{n} P_{fat}^{n} \left(1 - P_{fat}\right)^{N-n} \tag{12}$$

The search rate is

$$v_s = \frac{1}{T_I\left(1 + N P_{fat}\right)} \tag{13}$$

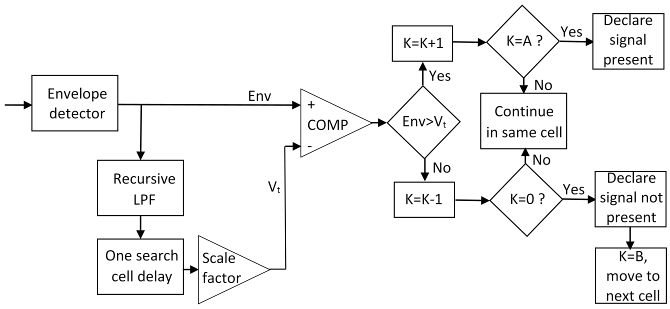

Fig. 5. Tong algorithm flowchart.

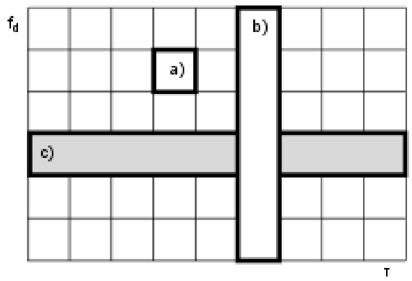

Fig. 6. Methods of the investigation of the search space, a) serial search, b) parallel search in Doppler frequency, c) parallel search in frequency domain.

For example, if the detection threshold is setup on $V_t = 2_n$, the $P_{fat} = 0.13$ and probability of the detection of the signal of $C/N_0 = 37dBc - Hz$ is $P_{dt} = 0.95$. The overall probability of signal detection after using the 6 of 8 algorithm is $P_{dNM} = 0.94$, the overall probability of false alarm is $P_{faNM} = 1.4 \cdot 10^{-5}$ and search rate is $v_s = 556 \, \frac{cells}{s}$. From the numerical example, it is clear, that M of N algorithm is highly effective due to the non-constant investigation time of the search cell.

The Tong algorithm is described by the flowchart in Fig. 5 [7], [9], The key block is the counter K, that is increased if the signal exceeds threshold and decrease in opposite case. The initial value of the counter B and threshold value A are the algorithm parameters that controls the search sensitivity and speed.

B. Parallel Search Method

In Fig. 6, there is a comparison of the most common acquisition methods [10]–[12]. The block diagram of the algorithm for parallel search in the frequency domain is on Fig. 7 and the block diagram of the algorithm for the parallel search in time (ranging code phase) domain is in Fig. 8.

The parallel search algorithm in frequency domain multiplies the signal by the replica. The output is not processed by the accumulator as in s classic GNSS correlator, but it is processed by the Fourier transform block of length M. The Fourier transform realizes not only accumulation but also multiplication (mixing) by the complex harmonic signal. In the FFT output, there are accumulated values for M frequency bins.

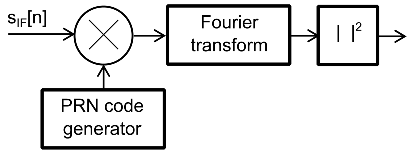

Fig. 7. Block diagram of the parallel Doppler frequency search algorithm.

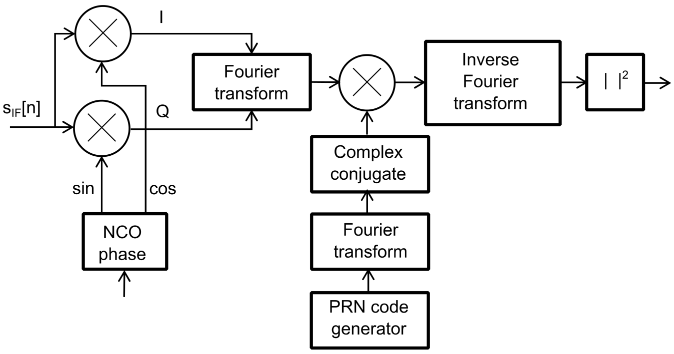

Fig. 8. Block diagram of the parallel code phase search algorithm.

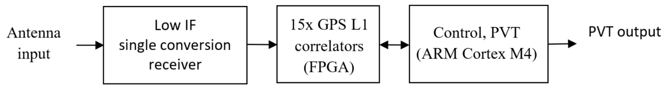

Fig. 9. piNAV L1 block diagram.

Fig. 10. piNAV L1 photo.

The parallel search in time domain calculates cross correlation function in spectral domain. The complex envelope signal is transformed to the spectral domain by the Fourier transform block, multiplied by the spectra of the replica signal and transformed back to the time domain by the inverse Fourier transform block.

There are also the numerically effective algorithms like Modified Double-Block Zero-Padding (MDBZP) algorithm [13] that can calculate the cross-correlation function for such search space, but their usage for a tiny space GPS receiver are problematic, because these algorithms require large portion of memory and they are algorithmically complicated and therefore not suitable for the low complexity FPGAs or processors that are used in pico-satellites.

IV. piNAV L1 GPS RECEIVER

piNAV L1 receiver is a GPS receiver (Fig. 9 and 10) developed for position determination of the small- and pico-satellites on LEO orbit. The receiver uses classic architecture of the GPS receiver, i.e. RF front end that uses modern low intermediated frequency receiver chip, a signal processor programmed to the low-power consumption FPGA, and a processor or microcontroller for receiver control and navigation task solution. The first version of the receiver is equipped with 15 GPS L1 correlators implemented to the FPGA. The receiver uses the M of N serial search algorithm. The performance of the algorithm was analyzed in [8]. The typical value of the cold start algorithm in LEO orbit is 300 seconds (5 minutes).

V. PROPOSED ACQUISITION ACCELERATOR

The acquisition accelerator can solve the main weakness of the piNAV receiver, which is a long cold start. The modern mass-market GPS receivers implement acquisition accelerator (unit) that shortens satellite signal search below one second. These accelerators are implemented into the ASICs, that are featured with high computation power. Unfortunately, these accelerators are optimized for mobile operation only and their reconfiguration, as well as reprogramming of the mass market receiver, is not possible as it is not allowed by the receiver producers.

The acquisition sensitivity of the space receiver can be obtained by the following consideration. There is a perfect view on the sky form the LEO satellite. The typical signal-to-noise ratios of the line of sight satellites lies between 43 and 50 dBc-Hz and higher [7]. The acquisition algorithm should guarantee high probability (at least 80%) of the signal detection for the signal with such. The implementation losses of the receiver hardware and software caused by the receiver noise, quantization noise, signal distortion etc. have to be respected. The typical value of the implementation losses is 3 – 6 dB [7].

The acquisition accelerator for the piNAV receiver should be applicable to the reasonably complex digital hardware while keeping low complexity, small size and light weight. The several implementation variants were analyzed, for example, processing of the signal snapshot in the digital signal processor (DSP) or digital signal microcontroller (DSM). Unfortunately, this solution cannot run in real time, so the signal snapshot of duration approximately 16 milliseconds must be preloaded to the memory. The processor should equiped with at least 64 kB of memory for the signal snapshot. The next memory is required for intermediate results etc. The lack of the internal memory of the low power DSP and DSM complicates the usability of such hardware design. In addition, the low-power consumption DSP or DSM has not enough performance, so the improvement is questionable.

The next analyzed variant, an implementation of the parallel code phase search algorithm to the low complexity FPGA is

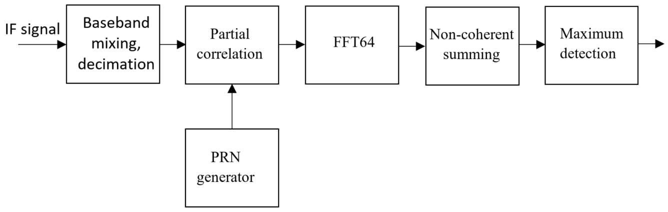

Fig. 11. Acquisition accelerator block scheme.

discouraged by the high memory requirement for the storage of the spectra of the replica signal and for the received signal sample as the low complex FFT algorithms do not process signal continuously but organize it to bursts.

The optimal algorithm for implementation of the cold start accelerator to the space receiver seems to be the parallel Doppler frequency search algorithm. The algorithm requires only one FFT block. The next reason for its selection is the wide Doppler frequency search range that is approximately five times wider than the search range of a standard GPS receiver. This simple algorithm improves significantly the acquisition time for the space GPS receiver.

The implemented acquisition accelerator (Fig. 11) executes parallel search space investigation in frequency and for all 32 PRN codes. The investigation in code phase delay runs sequentially. The required sensitivity for space operation is reached by non-coherent summing (section III) of the eight consecutive one millisecond time intervals. The proposed algorithm setup guarantees theoretical acquisition sensitivity approximately 34 dBc-Hz, see Fig. 4. The sensitivity after taking into the account 5 dB implementation losses is about 39 dBc-Hz. The total processing time of the whole search space for the all possible PRN codes is 20 seconds.

The first block of the realized acquisition accelerator transforms the signal to the baseband and reduces the sampling rate to the lowest required value with the aim to save computation demands. The partial correlator, PRN generator and FFT64 block realize parallel Doppler frequency search algorithm. In addition, the partial correlation block preprocess the signal for FFT64 block with the aim to set frequency search range to the required value.

The non-coherent summing block realizes the likelihood function (6) and the last block executes the search of its maximum.

As the accelerator is used only after power-up of the receiver, we have developed the following mode of the receiver operation Fig. 12. After power-on of the receiver, the acquisition accelerator is downloaded to the receiver FPGA. Then the accelerator is run. After 20 seconds, the coordinates of the correlation peaks of the individual PRN codes as well as the value of the cross-correlation function are sent to the receiver microcontroller. Then the FPGA is reprogrammed to contain the standard receiver correlators and the receiver performs a final search of the signals and starts to receive ephemeris of the acquired satellites. When the ephemeris of at least four satellites is received, the receiver starts to calculate position. The cold start time varies from 50 to 68 seconds.

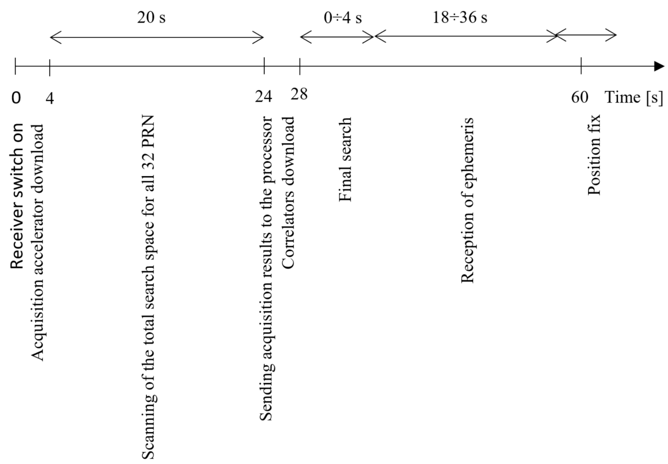

Fig. 12. Cold start time sequence.

The transmission time of ephemeris is 18 seconds, while the period of its retransmission is 30 seconds. In addition, we must consider the random duration of the final search that varies from 0 to 4 seconds.

The developed acquisition accelerator reduces the cold start time of the simple space GPS receiver approximately five times from 300 seconds to 60 seconds.

VI. Test Methodology and Results

The testing of the developed acquisition accelerator includes

1) Functional test in which the acquisition time and acquisition sensitivity were verified
2) Power and energy consumption of the piNAV receiver with implemented cold start accelerator

The test setup is in the Fig. 13. The test signal was generated by the software GPS simulator [6] and signal replayed. We used the radio transceiver based on software-defined radio (SDR) concept, capable of transforming signal samples to the radio signal or to convert radio signal to the digital form (signal samples). The signal level was controlled by the adjustable attenuator. The output signal from the attenuator is fed to the Pocket Cube version of the piNAV receiver that is placed in its evaluation kit. Two scenarios were used, the static scenario and the International Space Station (ISS) orbit. Static scenario generates navigation signals for fixed coordinates 14°00,0'E, 50°00,0'N. These results serve as a reference. The second scenario is the orbit of the ISS as an example of LEO orbit that is widely used by many small satellites as they are launched from ISS. The signal is affected by the Doppler shift typical for the LEO orbit.

The results of the acquisition time and sensitivity test are presented in the Table I. The simulator was set up to generate signals of 12 navigation satellites of the same signal to noise ratios C/N0. We measured the average number of satellites that were successfully acquired, and average cold start times were calculated from twenty attempts. The attempts were terminated after 70 seconds, so the higher sensitivity serial search method did not affect the results.

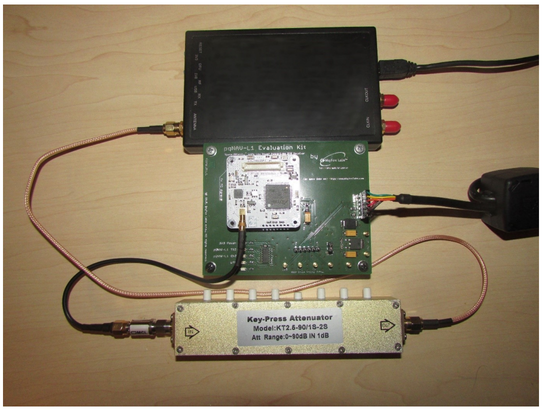

Fig. 13. piNAV receiver test setup.

TABLE I
COLD START TIME.

C/N_0 $[dBc-Hz]$	Static scenario		ISS scenario	
	Average number of acquired satellites	Average cold start time $[s]$	Average number of acquired satellites	Average cold start time $[s]$
44	9.6	61	8.9	61
43	8.1	61.5	7.7	62
42	7.0	62	6.8	63
41	5.4	64	5.1	64.5
40	4.6	64.5	4.2	64.5
39	4.1	65	3.9	No fix
38	3.2	No fix	2.8	No fix
37	0.8	No fix	0.4	No fix

The results of power and energy consumption tests are in the Tables II and III. Table II shows receiver supply current and energy consumption in the individual mode of operation. The total energy consumption to the position fix is analyzed in Table III.

TABLE II
RECEIVER SUPPLY CURRENT AT 3.3 V AND ENERGY CONSUMPTION.

Operation mode	Current $[mA]$	Duration $[s]$	Energy $[J]$
FPGA download	30	$2 \cdot 4$	0.792
Acquisition	50	20	3.3
Serial acquisition and tracking	36	-	0.12 per second of operation

The tests proved the expected cold start time and sensitivity of the acquisition accelerator. The cold start time is about 60 second, and the acquisition accelerator reliably processes the signal of 40 dBc–Hz so the sensitivity well corresponds with the theoretical expectations. In addition, if the acquisition unit fails, the receiver uses standard serial search method of the first version of the piNAV receiver with the sensitivity of approximately 38 dBc-Hz.

The differences between the static scenario and dynamic ISS scenario are very small. According to the expectations, the dynamic scenario seems to be of approx. 1 dB worse than the static one. The difference can be explained by higher implementation losses of the Doppler frequency search algorithm for the signal with higher Doppler frequency.

TABLE III
COLD START ENERGY CONSUMPTION.

Operation mode	I. version [J] (serial acquisition)	II. version [J] (accelerator)
Acquisition	-	3.3
Serial acquisition in reduced space and tracking (Ephemeris reception t = 30s)	-	3.6
Serial acquisition and tracking t = 300 s	36	-
Total	36	7.7

Let us note that the C/N0 of the unblocked GPS signal is typically better than 47 dBc-Hz for a satellite under 5° elevation mask and for a standard patch GPS antenna.

The power consumption calculated from the supply current when the acquisition unit is working is approximately 160 milliwatts, but it runs only 20 seconds after receiver power-up. After the reprogramming of the FPGA by the GPS correlators, the power consumption drops to 120 milliwatts.

The cold start energy consumption of the receiver is therefore reduced approximately 4.5 times and the acquisition time approximately 5 times.

VII. CONCLUSIONS

The paper describes the original method of the acceleration of the cold start of the LEO satellite GPS navigation receiver. The method was developed for the low complexity piNAV GPS L1 software receiver. The developed method was implemented into the receiver, tested and compared with the standard serial search method.

The tests have shown that the developed accelerator can shorten the cold start time of the receiver approximately 5 times. Energy usage for the position fix is reduced from 36 to 7.7 Joules (approx. 4.5 times). The sensitivity of the developed acquisition algorithms deteriorates of 4 dB to the original serial search algorithm, but the reached sensitivity of the algorithm is sufficient for a space operation with unblocked signal reception. The standard serial search acquisition algorithm is still kept in the receiver as a backup solution and is activated if the acquisition accelerator fails.

The reduction of the cold start time and cold start energy consumption enables new applications of the piNAV GPS L1 receiver in small Pocket Cube or femto-satellites in which the energy consumption of the navigation sensor is critical.

REFERENCES

[1] O. Montenbruck, M. Garcia-Fernandez, and J. Williams. Performance comparison of semicodeless GPS receivers for LEO satellites. *GPS Solutions*, 10(4):249–261, Mar. 2006.

[2] J. Yuan, H. Jia, and Q. Fang. Application of GPS to space vehicles: analysis of space environment and errors. *IEEE Aerospace and Electronic Systems Magazine*, 13(1):25–30, 1998.

[3] S. S. Arnold, R. Nuzzaci, and A. Gordon-Ross. Energy budgeting for CubeSats with an integrated FPGA. In *2012 IEEE Aerospace Conference*. IEEE, Mar. 2012.

[4] I. Ali, N. Al-Dhahir, and J.E. Hershey. Doppler characterization for LEO satellites. *IEEE Transactions on Communications*, 46(3):309–313, Mar. 1998.

[5] L. Sihver, S. Kodaira, I. Ambrozova, Y. Uchihori, and V. Shurshakov. Radiation environment onboard spacecraft at LEO and in deep space. In *2016 IEEE Aerospace Conference*. IEEE, Mar. 2016.

[6] T. Tsujii I. G. Petrovski. *Digital Satellite Navigation and Geophysics*. Cambridge University Press, 2012.

[7] E. D. Kaplan. *Understanding GPS: Principles and Applications, Second Edition*. Artech House, 2005.

[8] P. Kovar and S. Jelen. Cold start strategy of the CubeSat GPS receiver. *Advances in Electrical and Computer Engineering*, 14(2):29–34, 2014.

[9] J. Walker. Performance data for a double-threshold detection radar. *IEEE Transactions on Aerospace and Electronic Systems*, AES-7(1):142–146, jan 1971.

[10] S. Yuyao, W. Yongqing, C. Jingyao, and W. Siliang. High sensitivity acquisition algorithm for DSSS signal with data modulation. *China Communications*, 12(4):76–85, Apr. 2015.

[11] D. J. R. van Nee and A. J. R. M. Coenen. New fast GPS code-acquisition technique using FFT. *Electronics Letters*, 27(2):158, 1991.

[12] P. W. Ward. GPS receiver search techniques. In *Proceedings of Position, Location and Navigation Symposium - PLANS '96*. IEEE, 1996.

[13] W. Zhang and M. Ghogho. Improved fast modified double-block zero-padding (fmdbzp) algorithm for weak gps signal acquisition. In *2010 18th European Signal Processing Conference*, pages 1617–1621, Aug. 2010.